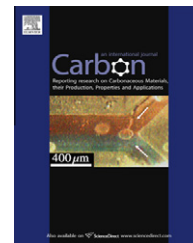


available at www.sciencedirect.comjournal homepage: www.elsevier.com/locate/carbon

Spinnable carbon nanotube forests grown on thin, flexible metallic substrates

Xavier Lepró, Márcio D. Lima^{*}, Ray H. Baughman

The University of Texas at Dallas, The Alan G. MacDiarmid NanoTech Institute, BE 26, 800 West Campbell Road, Richardson, TX 75083, USA

ARTICLE INFO

Article history:

Received 18 March 2010

Accepted 8 June 2010

Available online 11 June 2010

ABSTRACT

Towards the goal of providing a continuous process for the solid-state fabrication of carbon nanotube sheets and yarns from carbon nanotube forests, we report the growth of yarn-spinnable and sheet-drawable carbon nanotube forests on highly flexible stainless steel sheets, instead of the conventionally used silicon wafers. Sheets and yarns were fabricated from the 16 cm maximum demonstrated forest width, from both sides of a stainless steel sheet, and the catalyst layer was shown to be reusable, thereby decreasing the need for catalyst renewal during a proposed continuous or semi-continuous process where the stainless steel sheet serves as a moving belt to enable forest growth at one belt end and carbon nanotube yarn or sheet fabrication at an opposite belt end.

© 2010 Elsevier Ltd. All rights reserved.

1. Introduction

Individual carbon nanotubes (CNTs) have been long well known to have exceptional mechanical, electronic, photonic, and optical properties, which could provide important applications for both nanoscale devices and macroscopic applications [1]. For macroscopic applications there is the need to assemble these CNTs into yarns and sheets at commercially acceptable costs, while minimizing the properties degradation in going from individual CNT characteristics to those of the yarns and sheets. To understand the scale of the problem, several billion miles of typical 10 nm diameter, 10 wall CNTs must be assembled for every pound of produced sheet or yarn – and the miles needed increases with decreasing CNT diameter and number of walls. Alternative fabrication processes include, for example, solution-state spinning [2–5], assembly of gas phase synthesized CNTs [6,7], and solid-state spinning from CNT forests [8–16]. CNT forests (also called CNT carpets) superficially resemble bamboo forests, except that the CNT “trees” in these forests can be over 50,000 times longer than

their diameter, and this very high aspect ratio is useful for optimizing properties.

We focus on advancing solid-state spinning from CNT forests towards large scale commercial applications. Solution-based technologies are limited by the length of CNTs that can be processed, which can decrease length-dependent properties like electrical and thermal conductivities and mechanical strength and modulus. Technologies using pre-synthesis of CNTs in the gas phase before structural assembly into yarns or sheets have the problem that the initially collected CNT assemblies are disordered, and it is challenging to introduce a high degree of CNT alignment during post processing. The process that is probably most advanced towards achieving commercial scale production employs gas phase synthesis using the floating catalyst method, CNT collection as a disordered array, and subsequent mechanical processing to achieve useful CNT orientation [6,7].

CNT-forest-based spinning on the commercial scale provides difficult challenges, which we presently help address. More specifically, the research goal is to replace the presently

^{*} Corresponding author: Fax: +1 972 883 6529.

E-mail address: marciodiaslima@gmail.com (M.D. Lima).

0008-6223/\$ - see front matter © 2010 Elsevier Ltd. All rights reserved.

doi:10.1016/j.carbon.2010.06.016

used silicon substrates for forest growth with inexpensive metal sheets that could serve as continuous belts, where at one belt end the CNTs are grown in the furnace and at an opposite belt end the forests are converted by drawing into CNT yarns or sheets. Since few methods for growing CNT forests result in forest drawability, the challenge is to discover forest growth methods that both work for metal sheet substrates and provide the very limited range of forest topology that enables forest drawability.

Until now several successful efforts to obtain CNTs on metallic substrates have been reported [17–19]. Particularly, for those focused on achieving CNT growth on stainless steel (SS) substrates the strategies have been based in adapting either traditional chemical vapor deposition (CVD) [20], plasma enhanced CVD (PECVD) [21–25] or floating catalyst CVD techniques [26,27] which are robust enough to obtain CNTs forests grown directly on the inner surface of SS tubing [28]. Increased CNT alignment and uniformity for CNT forests grown on metal substrates resulted from process developments for seeded catalyst CVD and floating catalyst CVD [26,29]. Further improvements were obtained when catalyst particles or films were deposited on metal sheets previously coated with thin ceramic buffer layers, such as alumina (Al_2O_3), silicon nitride (Si_3N_4) and indium tin oxide ($\text{In}_2\text{O}_3:\text{Sn}$) which act as interfacial agent for CNT growth [30,31]. In addition to multi-walled CNTs (MWCNTs), double-walled (DWCNTs), single-walled CNTs (SWCNTs) [32] and mixed arrays of MWCNTs and SWCNTs [33] have been grown on metal substrates.

Despite these successes, we have not found a report for the growth of spinnable CNT forests on a metal substrate. This apparent absence of reports of forest spinnability for CNTs grown on metal substrates is not surprising, because of the special CNT forest topology needed for spinnability. Seemingly extremely minor changes in CNT forests synthesis conditions result in a change from highly spinable CNT forests to unspinnable ones. Only few groups have reported the synthesis of spinnable CNT forests [8–16], though many more teams have been in pursuit of this goal. On the other hand, when the host of interrelated synthesis conditions is properly set (which depends on furnace type, surrounding thermal environment, provided thermal gradients, temperatures, gas flow conditions, catalyst type and pretreatments) highly drawable CNT forests can be obtained reproducibly and qualitatively.

In this letter we report a suitable method to produce these dry-state spinnable CNT forests on commercial thin sheets of SS that are flexible enough to be elastically bent into a small radius and can be easily cut by regular scissors (both before and after application of surface layers and growth of drawable CNT forest). The yarns and sheets that we can produce from these CNT forests provide interesting electronic [8,9,34–36] and mechanical properties [9–11] that could be deployed for structural applications and for such novel uses as transparent conducting films, polarizers, polarized light sources, and organic light emitting diodes, [10] charge strippers for ion accelerators [37], thermoacoustic loudspeakers [38], artificial muscles [39,40], bolometers, and elements for conductive and irradiative heat dissipation [41].

For growing drawable CNT forests on inexpensive SS sheets the set of CVD parameters was narrowed to those that

have shown the successful growth of these kinds of CNT forests on Si wafers [9]. We focused on the study of the following factors: (1) the presence or absence of a buffer layer, its type (Al , Al_2O_3 , Si or SiO_x), and its thickness (~ 10 or ~ 100 nm); and regarding the synthesis process, (2) the presence or absence of H_2 during the heating of the substrate, which transforms the catalyst film to active catalyst nanoparticles; and (3) the hydrocarbon precursor used.

2. Experimental

2.1. Preparation of the substrate

Commercial SS foil (type 321, 50.8 μm thick. Nominal composition: 18% Cr, 9% Ni, 2% Mn, 1% Si and 0.1% C balanced with Fe) was first sequentially cleaned in an ultrasonic bath of distilled water, methanol (CH_3OH) and acetone ($(\text{CH}_3)_2\text{CO}$). Posterior to this cleaning, a buffer layer of either Al , Al_2O_3 , Si or SiO_x was deposited onto its surface. Two film thicknesses were used for comparison purposes: ~ 10 or ~ 100 nm. Al and Al_2O_3 were deposited by electron beam evaporation (EBE) measuring the deposited thickness by a quartz crystal monitor. Si and SiO_x films, on the other hand, were deposited by PECVD at 200 and 250 $^\circ\text{C}$, respectively using a RF power of 50 W. SiH_4 was used as silicon precursor, and a mixture of SiH_4 and N_2O was required for producing silicon oxide. In this case, ellipsometric measurements were performed to verify the accuracy of the thicknesses achieved. Finally, Fe catalyst was deposited as a layer of 2 nm thick by EBE.

2.2. Spinnable CNT synthesis

Two different carbon precursors were tested for CNT forest growth: acetylene (C_2H_2 , Air Liquide, >99.6%) and ethylene (C_2H_4 , Air Liquide, 99.995%). Similar CVD reactors (tubular quartz hot-wall, resistively heated furnaces, containing 65 and 72 mm inner diameter quartz tubes, respectively) were used for both carbon precursors. In the acetylene system (using 800 sccm Ar (Air Liquide, 99.999%) as carrier gas, 30 v% H_2 (Air Liquide, 99.999%) and 7 v% C_2H_2), the substrates were positioned on a special quartz holder that allows inserting and removing the samples from the hot zone of the CVD furnace (at 700 $^\circ\text{C}$) under a controlled, inert atmosphere. Besides argon, either N_2 or He can also be used as a carrier gas. The heat up and cool down was done in only 5 min by inserting and removing the samples in the already hot reactor. This procedure reduces drastically the total syntheses to only 15 min, what allowed approximately four forest synthesis runs per hour.

For CNT synthesis using ethylene the SS substrates were positioned inside the cold CVD reactor and then heated to the CNT synthesis temperature (760 $^\circ\text{C}$) for 15 min. The growth of CNT lasted for 10 min using typical conditions of growth (Ar as carrier gas, 20 v% H_2 and 10 v% C_2H_4) at a total flow of 1000 sccm. The CNTs and CNT forests morphologies obtained from both methods were further characterized by scanning electron microscopy, SEM (Zeiss Supra 40 and JEOL 2100F at 10–20 kV), transmission electron microscopy, TEM (JEOL 2100 at 200 kV) and Micro-Raman spectroscopy

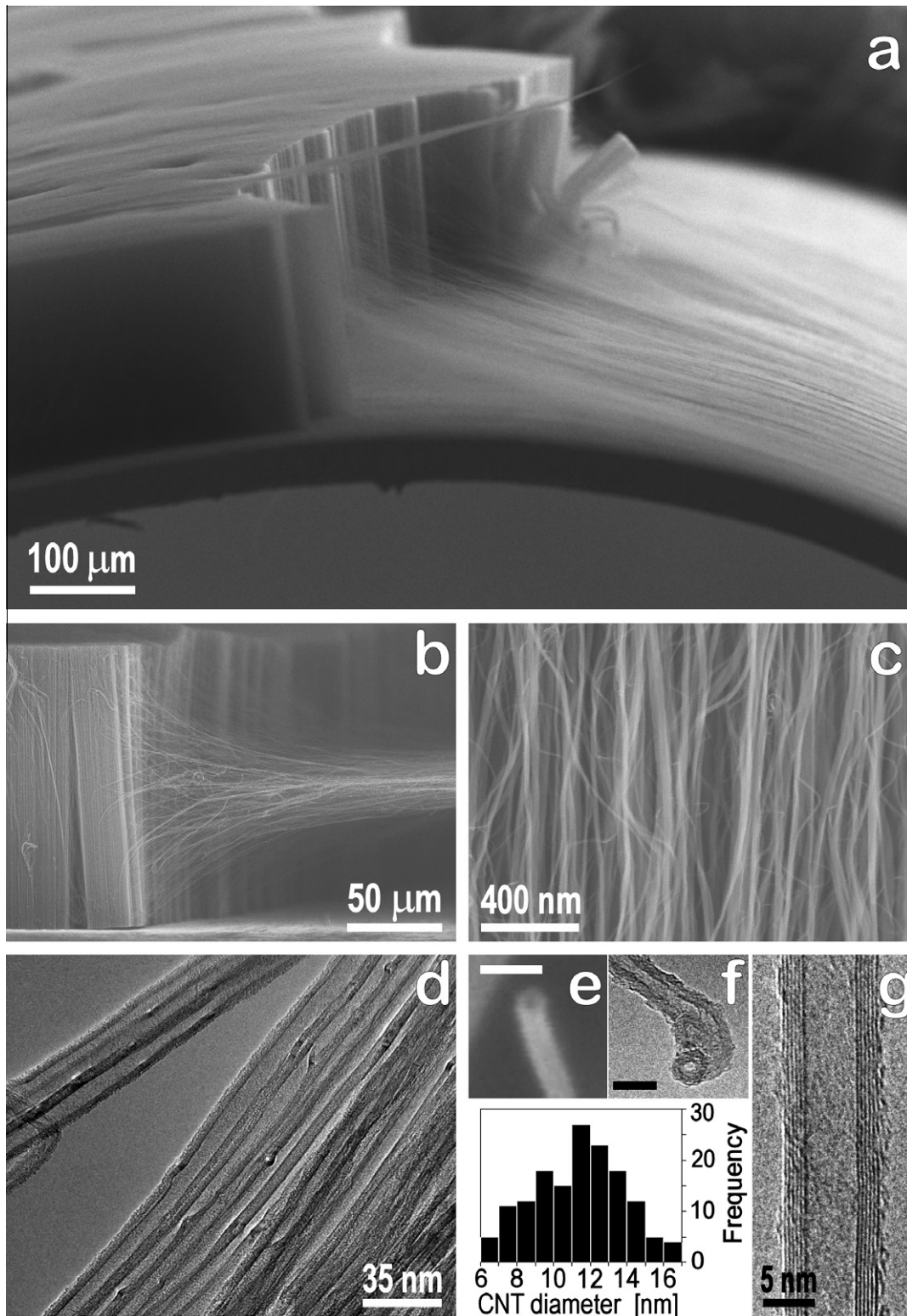


Fig. 1 – Electron microscopy images of drawable CNT forests grown on SS sheets: (a) low magnification SEM image of a CNT ribbon being drawn from a forest. The SS sheet substrate is bent to show that it still retains its elastic flexibility while enabling draw. (b) Cross-sectional view of the CNT forest's edge showing CNT self-assembly to form a sheet; (c) high magnification image showing the alignment of the CNTs in the forest side-wall. (d) TEM image of the aligned CNTs pulled from this forest and (right inset) its diameter distribution. (e) High magnification SEM (scale bar is 20 nm) and (f) TEM (scale bar is 10 nm) showing the open CNT roots after their removal from the substrate. (g) High resolution TEM image showing in detail one 6-walled CNT from the spinnable forest.

(Horiba Jobin Yvon LabRam HR Spectrometer using a He–Ne laser wavelength of 632.8 nm).

3. Results and discussion

For our specific synthesis conditions, the presence of a buffer layer has high impact on the CNT growth. Bare SS foil and SS foil with a thin film of iron deposited directly on its surface did not produce CNT forests. SS is well known to form a hard passivation layer of chromium oxide on its surface. Apparently, this oxide is not a proper substrate for the growth of CNTs in the range of temperature and gas mixtures tested. On the other hand, when a buffer layer between the catalyst film and the SS substrate was used, CNT growth was generally observed under the same synthesis conditions. These results on the production of CNT forests are consistent with those previously reported for non-spinnable forests [21,26,30,32,33,42].

Growth of homogeneous and aligned CNT forests was found to depend on the buffer layer material and, to some extent, its thickness. The four different types of buffer layers tested: Al, Al₂O₃, Si and SiO_x were selected for evaluation because the first two are usual buffer layers for the growth of

vertically aligned CNTs on silicon substrates [30], while the last two were intended to chemically simulate the surface of a silicon wafer. From the extreme buffer layers thicknesses tested, i.e. ~10 and ~100 nm, the ones of 100 nm generally produced higher quality forests. Additionally, exclusion of H₂ during the heating of the substrate, before the injection of the hydrocarbon, provided improved CNT growth for the range of temperatures (700–760 °C) and gas mixtures evaluated.

Ethylene and acetylene were separately used as carbon precursor gases in order to compare their relative effectiveness for CNT growth. Using ethylene, all four buffer layers produced CNT forests. Aluminum and SiO_x buffer layers provided the more homogeneous and taller forests, ~40 μm within 10 min, compared with ~20 and ~10 μm high forests in the same time period for Al₂O₃ and Si barrier layers. Using longer synthesis times (30 min), ~1 mm tall CNTs forests were grown using Al as buffer layer. For acetylene as carbon source gas, the oxide buffer layers were slightly better for producing tall, homogenous CNT forests (judged by the naked eye) than Si or Al buffer layers, but high quality drawable CNT forests were achieved only by using SiO_x as buffer material. However we

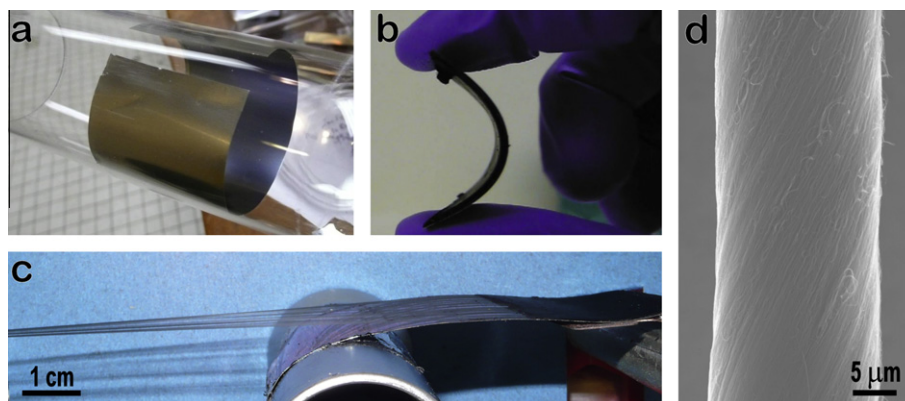


Fig. 2 – Flexibility of the SS substrate. Flexibility of the SS substrate before and after thermal CVD CNT forest growth: (a) a SS foil bent on the inner surface of the quartz tube (inner diameter, ca. 65 mm) used as a reactor chamber before to be submitted to the CVD thermal process. (b) Piece of a forest growth on a SS foil being elastically bent. (c) Photograph of a 5 cm wide CNT sheet being pulled from a forest growth on a bent SS substrate. (d) SEM image of a CNT yarn spun from a forest growth on SS.

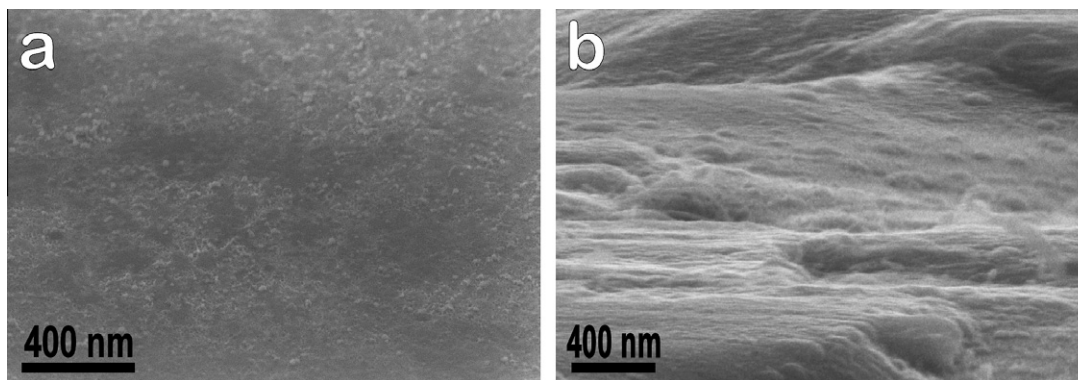


Fig. 3 – Roughness of different kinds of substrates after removing the spinnable CNT forests: (a) a flat Si wafer substrate and (b) the surface of a SiO_x buffer layer coated SS sheet. Both pictures were taken on samples tilted ~30° from the normal to the SEM detector.

do not discard the possibility of achieving spinnable forests using the other buffer layers tested here as well after further tuning the synthesis conditions for these materials.

In general, the use of acetylene as carbon precursor and silicon oxide buffer layer enabled the production of the most highly spinnable and drawable CNT forests, importantly without decreasing the elastic flexibility of the SS sheet substrate. This last factor can be important for applications of this process where the substrate itself can act as a belt for continuous or semi-continuous CNT yarn or sheet production. These CNT forests growth on SS foil can be as easily spun in the solid-state as those successfully produced on highly flat Si wafers [9,10]. Moreover, wide CNT sheets (from forests produced on areas of up to 16 cm by 12 cm) could be drawn from this highly flexible SS substrate (Fig. 1a).

SEM images of the self-assembly process that converts CNT forests grown on SS to aligned CNT sheets (see Fig. 1b) show a similar structure to that we have previously observed for drawable CNT forests grown on Si wafers [9,10]. High magnification SEM micrograph of the forest side-wall (Fig. 1c), shows the alignment of CNTs in the spinnable forest. This alignment seems to play an important role for spinnability. Very waived CNTs, in general, tend to decrease or completely suppress the spinnability of a forest. Diameter of the CNTs in this forest is around 11.1 ± 2.4 nm, according to TEM observations (Fig. 1d and inset). Fig. 1e shows a SEM view of the roots of the CNT forest after being removed from the substrate.

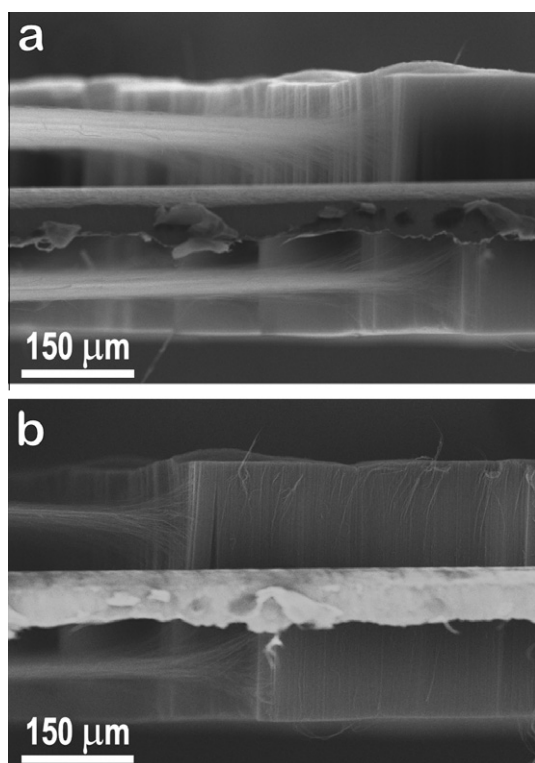


Fig. 4 – SEM images of CNT sheets being simultaneously drawn from CNT forests grown on both sides of a SS sheet: (a) image obtained using the secondary electron (SE) detector and (b) image obtained using the TLD (Through Lens Detector), showing the transitional structure formed during sheet draw.

TEM observation at those roots (see Fig. 1f) shows that these CNTs are mostly open, without visible remainders of catalytic particles. High resolution TEM imaging displays the structures of the CNTs produced (see Fig. 1g).

Fig. 2a shows a 16 cm long, 12 cm wide SS sheet substrate that has been bent longitudinally, so that it fits neatly within a 65 mm diameter quartz furnace tube (with catalyst and buffer layer on the interior side). Homogeneous, highly spinnable forest grew over this 12 cm by 16 cm area. The use of such easily configurable SS substrate, as opposed to a rigid Si substrate, enabled to increase the forest production of wide substrates per batch in our furnace by a factor of about π , and more generally avoids the cost and wafer size restrictions of commercially available Si wafers. Since the SS substrate remains highly flexible after the CNT forest growth, as shown by Fig. 2b, it is possible to bend the as-produced forest around small diameter (2.5 cm) mandrels while a CNT sheet is drawn from it (Fig. 2c), thereby expanding the geometries and dimensions that can be used for yarn and sheet fabrication from forests. The single-ply yarns prepared from spinning these forests (Fig. 2d) exhibit values of electrical conductivity and tensile strengths of 350 S/cm and 303 MPa, respectively, which are not substantially different from reported values [9] for CNT yarns fabricated from forests growth on Si substrates. Consequently, the SS substrates appear well suited for use as a conveyor belt substrate for the upscaled production of CNT yarns and sheets by a continuous or semi-continuous CNT forest growth process, where the forest growth and forest stripping as yarn or sheet could be started at different regions of the SS belt.

Surprisingly, the forest spinnability is insensitive to the surface roughness of our SS sheets, which is why we could use commercially purchased SS wrapping foil as substrates. After forest growth, the forest was removed from the SS and Si substrates in order to analyze their relative surface roughness. SEM images (Figs. 3a and b) compare the post-synthesis surface morphology of a Si wafer substrate and a SS sheet (subjected to the same CNT synthesis conditions and both coated with ~ 100 nm of SiO_x buffer layer). While the SS sheet has a much rougher surface structure than the Si wafer, there

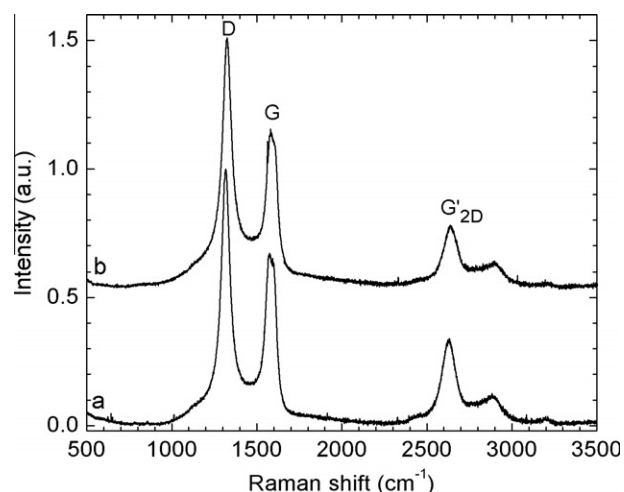


Fig. 5 – Raman spectra of (a) unspinnable CNT forests and (b) spinnable forest growth on SS.

was no noticeable difference in the drawability of the produced forests.

We also found that the forest area available from a run can be doubled without sacrifice of forest drawability by depositing the buffer and catalytic layers on both faces of the metallic foil. Simultaneous sheet drawn from opposite sides of a SS sheet is shown in Fig. 4a and b. In this instance, CNT forests height (~160 μm) was three times higher than the thickness of the SS foil. Conductivity tests showed the existence of electrical contact between the SS substrate and the top of the drawable forests, despite the thin insulator film used as a buffer layer for the CNT growth. Potential applications of these spinnable forests on SS sheets can include field emission [43], thermal dissipation [41] and electrochemical applications [27,44,45].

Unless the initially deposited catalyst layer can be reused, either catalyst renewal or continuous feed of new SS foil into the CVD reactor will be needed. Our preliminary study (for iron catalyst on a SiO_x buffer layer and acetylene feedstock gas) showed that the catalyst was active to provide spinnable forests for two cycles without renewing the buffer layer or catalyst. Though forests can be produced during a subsequent third cycle, these are not spinnable. This lack of spinnability for the third produced forest might be due to partial catalyst deactivation or partial catalyst removal during consecutive cycles of forest spinning. However, CNT re-growth indicates that a considerable amount of catalytic active nanoparticles remain attached to the buffer layer during the synthesis process of CNTs, suggesting a base-growth process. The requirements for sheet spinnability and drawability are complex, and related to details of forest structure, like CNT density, mechanical modulus, alignment and the degree of entanglement between CNTs. Raman spectroscopy performed on both unspinnable and spinnable forests (see Fig. 5) do not show important differences that can be readily related to morphological differences in the CNTs or forests.

The inability to spin forest produced in the third above cycle likely resulted from decreased forest density, but further studies are needed to understand the transition from drawable to unspinnable forests when the catalytic substrates are reused for CNT growth.

4. Conclusions

In this paper, we presented a method to produce drawable CNT forests in dry state using substrates other than the usual Si wafers. By the correct selection of buffer layers, carbon precursors and synthesis conditions, the growth of CNT forests can be achieved in thin SS metallic foils (50 μm thick) which might be extended to other kind of materials and substrates. In our case the best set of conditions included the use of a SiO_x buffer layer together with acetylene as carbon precursor.

The retained mechanical flexibility of the SS sheets after the CNT drawable forest synthesis and its low cost (at least 60 times cheaper per area than Si wafers), are important considerations for their use as belts for continuous or semi-continuous CNT yarn and sheet production from forests. The advances made here will likely be important for upscale of forest-based yarn and sheet production and to get a further understanding of the key parameters involved in the growth

of drawable CNT forests. The results here found are encouraging to further pursue the growth of these forests on substrates and geometries different to the ones we have been restricted so far.

Acknowledgements

The authors thank to Dr. Raquel Ovalle Robles for her helpful discussions and suggestions. This work was supported by Office of Naval Research Grants STTR N00014-08-M-0323 and MURI N00014-08-1-0654, NSF Grant DMI-0609115, Robert A. Welch Foundation Grant AT-0029, and CONACYT-México-UTD (for the Ph.D. scholarship of X.L.).

REFERENCES

- [1] Baughman RH, Zakhidov AA, de Heer WA. Carbon nanotubes – the route toward applications. *Science* 2002;297:787–92.
- [2] Vigolo B, Penicaud A, Coulon C, Sauder C, Paillet R, Journet C, et al. Macroscopic fibers and ribbons of oriented carbon nanotubes. *Science* 2000;290:1331–4.
- [3] Ericson LM, Fan H, Peng HQ, Davis VA, Zhou W, Sulpizio J, et al. Macroscopic, neat, single-walled carbon nanotube fibers. *Science* 2004;305(5689):1447–50.
- [4] Kumar S, Dang TD, Arnold FE, Bhattacharyya AR, Min BG, Zhang XF, et al. Synthesis, structure, and properties of PBO/SWNT composites. *Macromolecules* 2002;35(24):9039–43.
- [5] Dalton AB, Collins S, Munoz E, Razal JM, Ebron VH, Ferraris JP, et al. Super-tough carbon-nanotube fibres – these extraordinary composite fibres can be woven into electronic textiles. *Nature* 2003;423(6941):703.
- [6] Li YL, Kinloch IA, Windle AH. Direct spinning of carbon nanotube fibers from chemical vapor deposition synthesis. *Science* 2004;304(5668):276–8.
- [7] Lashmore DS, Braden R, Hart AJ, Welch J. Chemically-assisted alignment of nanotubes within extensible structures. US Patent 2009029341; 2009.
- [8] Jiang KL, Li QQ, Fan SS. Nanotechnology: spinning continuous carbon nanotube yarns – carbon nanotubes weave their way into a range of imaginative macroscopic applications. *Nature* 2002;419(6909):801.
- [9] Zhang M, Atkinson KR, Baughman RH. Multifunctional carbon nanotube yarns by downsizing an ancient technology. *Science* 2004;306:1358–61.
- [10] Zhang M, Fang S, Zakhidov AA, Lee SB, Aliev AE, Williams CD, et al. Strong, transparent, multifunctional, carbon nanotube sheets. *Science* 2005;309:1215–9.
- [11] Li Q, Zhang X, DePaula RF, Zheng L, Zhao Y, Stan L, et al. Sustained growth of ultralong carbon nanotube arrays for fiber spinning. *Adv Mater* 2006;18:3160–3.
- [12] Zhang S, Zhu L, Minus ML, Chae HG, Jagannathan S, Wong CP, et al. Solid-state spun fibers and yarns from 1-mm long carbon nanotube forests synthesized by water-assisted chemical vapor deposition. *J Mater Sci* 2008;43(13):4356–62.
- [13] Liu K, Sun YH, Chen L, Feng C, Feng XF, Jiang KL, et al. Controlled growth of super-aligned carbon nanotube arrays for spinning continuous unidirectional sheets with tunable physical properties. *Nano Lett* 2008;8(2):700–5.
- [14] Nakayama Y. Synthesis, nanoprocessing, and yarn application of carbon nanotubes. *Jpn J Appl Phys, Part 2* 2008;47(10):8149–56.
- [15] Mallik N, Schulz MJ, Shanov VN, Hurd D, Chakraborty S, Jayasinghe C, et al. Study on carbon nano-tube spun thread

- as piezoresistive sensor element. *Adv Mater Res* 2009;67:155–60.
- [16] Tran CD, Humphries W, Smith SM, Huynh C, Lucas S. Improving the tensile strength of carbon nanotube spun yarns using a modified spinning process. *Carbon* 2009;47(11):2662–70.
- [17] Du CS, Pan N. CVD growth of carbon nanotubes directly on nickel substrate. *Mater Lett* 2005;59(13):1678–82.
- [18] Reddy NK, Meunier JL, Coulombe S. Growth of carbon nanotubes directly on a nickel surface by thermal CVD. *Mater Lett* 2006;60(29–30):3761–5.
- [19] Talapatra S, Kar S, Pal SK, Vajtai R, Ci L, Victor P, et al. Direct growth of aligned carbon nanotubes on bulk metals. *Nat Nanotechnol* 2006;1(2):112–6.
- [20] Vander Wal RL, Hall LJ. Carbon nanotube synthesis upon stainless steel meshes. *Carbon* 2003;41(4):659–72.
- [21] Park D, Kim YH, Lee JK. Pretreatment of stainless steel substrate surface for the growth of carbon nanotubes by PECVD. *J Mater Sci* 2003;38(24):4933–9.
- [22] Lin CL, Chen CF, Shi SC. Field emission properties of aligned carbon nanotubes grown on stainless steel using CH₄/CO₂ reactant gas. *Diamond Relat Mater* 2004;13(4–8):1026–31.
- [23] Hu JJ, Jo SH, Ren ZF, Voevodin AA, Zabinski JS. Tribological behavior and graphitization of carbon nanotubes grown on 440C stainless steel. *Tribol Lett* 2005;19(2):119–25.
- [24] Abad MD, Sánchez-López JC, Berenguer-Murcia A, Golovko VB, Cantoro M, Wheatley AEH, et al. Catalytic growth of carbon nanotubes on stainless steel: characterization and frictional properties. *Diamond Relat Mater* 2008;17(11):1853–7.
- [25] Park D, Hoon Kim Y, Kee Lee J. Synthesis of carbon nanotubes on metallic substrates by a sequential combination of PECVD and thermal CVD. *Carbon* 2003;41(5):1025–9.
- [26] Masarapu C, Wei BQ. Direct growth of aligned multiwalled carbon nanotubes on treated stainless steel substrates. *Langmuir* 2007;23(17):9046–9.
- [27] Yun Y, Gollapudi R, Shanov V, Schulz MJ, Dong ZY, Jazieh A, et al. Carbon nanotubes grown on stainless steel to form plate and probe electrodes for chemical/biological sensing. *J Nanosci Nanotechnol* 2007;7(3):891–7.
- [28] Karwa M, Iqbal Z, Mitra S. Scaled-up self-assembly of carbon nanotubes inside long stainless steel tubing. *Carbon* 2006;44(7):1235–42.
- [29] Pal SK, Talapatra S, Kar S, Ci L, Vajtai R, Borca-Tasciuc T, et al. Time and temperature dependence of multi-walled carbon nanotube growth on Inconel 600. *Nanotechnology* 2008;19(045610):1–5.
- [30] Parthangal PM, Cavicchi RE, Zachariah MR. A generic process of growing aligned carbon nanotube arrays on metals and metal alloys. *Nanotechnology* 2007;18(185605):1–5.
- [31] García-Céspedes J, Thomasson S, Teo KBK, Kinloch IA, Milne WI, Pascual E, et al. Efficient diffusion barrier layers for the catalytic growth of carbon nanotubes on copper substrates. *Carbon* 2009;47(3):613–21.
- [32] Hiraoka T, Yamada T, Hata K, Futaba DN, Kurachi H, Uemura S, et al. Synthesis of single- and double-walled carbon nanotube forests on conducting metal foils. *J Am Chem Soc* 2006;128(41):13338–9.
- [33] Qu L, Dai L. Direct growth of three-dimensional multicomponent micropatterns of vertically aligned single-walled carbon nanotubes interposed with their multi-walled counterparts on Al-activated iron substrates. *J Mater Chem* 2007;17(32):3401–5.
- [34] Zakhidov AA, Nanjundaswamy R, Obraztsov AN, Zhang M, Fang S, Klesh VI, et al. Field emission of electrons by carbon nanotube twist-yarns. *Appl Phys A: Mater Sci Process* 2007;88:593–600.
- [35] Williams CD, Robles RO, Zhang M, Li S, Baughman RH, Zakhidov AA. Multiwalled carbon nanotube sheets as transparent electrodes in high brightness organic light-emitting diodes. *Appl Phys Lett* 2008;93(183506):1–3.
- [36] Atkinson KR, Hawkins SC, Huynh C, Skourtis C, Dai J, Zhang M, et al. Multifunctional carbon nanotube yarns and transparent sheets: fabrication, properties, and applications. *Physica B* 2007;394(2):339–43.
- [37] von Reden K, Zhang M, Meigs M, Sichel E, Fang SL, Baughman RH. Carbon nanotube foils for electron stripping in tandem accelerators. *Nucl Instrum Methods Phys Res, Sect B* 2007;261(1–2):44–8.
- [38] Xiao L, Chen Z, Feng C, Liu L, Bai ZQ, Wang Y, et al. Flexible, stretchable, transparent carbon nanotube thin film loudspeakers. *Nano Lett* 2008;8(12):4539–45.
- [39] Ebron VH, Yang ZW, Seyer DJ, Kozlov ME, Oh JY, Xie H, et al. Fuel-powered artificial muscles. *Science* 2006;311(5767):1580–3.
- [40] Aliev AE, Oh JY, Kozlov ME, Kuznetsov AA, Fang SL, Fonseca AF, et al. Giant-stroke, superelastic carbon nanotube aerogel muscles. *Science* 2009;323:1575–8.
- [41] Aliev AE, Guthy C, Zhang M, Fang S, Zakhidov AA, Fischer JE, et al. Thermal transport in MWCNT sheets and yarns. *Carbon* 2007;45(15):2880–8.
- [42] Somchai T, Singjai P, Mai C. Growth of CNTs on 304 stainless steel using sparked iron as a catalyst. *Mater Sci Forum* 2006;510–511:470–3.
- [43] Rao AM, Jacques D, Haddon RC, Zhu W, Bower C, Jin S. *In situ*-grown carbon nanotube array with excellent field emission characteristics. *Appl Phys Lett* 2000;76(25):3813–5.
- [44] Niu CM, Sichel EK, Hoch R, Moy D, Tennent H. High power electrochemical capacitors based on carbon nanotube electrodes. *Appl Phys Lett* 1997;70(11):1480–2.
- [45] Gao LJ, Peng AP, Wang ZY, Zhang H, Shi ZJ, Gu ZN, et al. Growth of aligned carbon nanotube arrays on metallic substrate and its application to supercapacitors. *Solid State Commun* 2008;146:380–3.